


Assessment of early diastolic intraventricular pressure gradient in the left ventricle among patients with repaired tetralogy of Fallot

Maki Kobayashi¹ · Ken Takahashi¹  · Mariko Yamada¹ · Kana Yazaki¹ · Kotoko Matsui² · Noboru Tanaka² · Sachie Shigemitsu² · Katsumi Akimoto² · Masahiko Kishiro² · Keisuke Nakanishi³ · Shiori Kawasaki³ · Masaki Nii⁴ · Keiichi Itatani⁵ · Toshiaki Shimizu¹

Received: 5 February 2017 / Accepted: 16 June 2017 / Published online: 20 June 2017
© Springer Japan KK 2017

Abstract Assessment of left ventricular (LV) dysfunction is vital in patients with repaired tetralogy of Fallot (rTOF). The early diastolic intraventricular pressure gradient (IVPG) in the LV plays an important role in diastolic function. IVPG is calculated as the intraventricular pressure difference divided by the LV length, which allows to account for differences in LV size and therefore calculate IVPG in children. We aimed to investigate the mechanisms of LV diastolic dysfunction by measuring mid-to-apical IVPG as an indicator of the active suction force sucking blood from the left atrium into the LV. We included 38 rTOF patients and 101 healthy controls. The study population was stratified based on age group into children (4–9 years), adolescents (10–15 years), and adults (16–40 years). IVPGs were calculated based on mitral inflow measurements obtained using color M-mode Doppler echocardiography. Although

total IVPGs did not differ between rTOF patients and controls, mid-to-apical IVPGs in adolescents and adults were smaller among rTOF patients than among controls (0.15 ± 0.05 vs. 0.21 ± 0.06 mmHg/cm, $p < 0.05$; 0.09 ± 0.07 vs. 0.17 ± 0.05 mmHg/cm, $p < 0.001$; respectively). Additionally, only mid-to-apical IVPG correlated linearly with peak circumferential strain ($\rho = 0.217$, $p = 0.011$), longitudinal strain ($\rho = -0.231$, $p = 0.006$), torsion ($\rho = -0.200$, $p = 0.018$), and untwisting rate in early diastole ($\rho = -0.233$, $p = 0.006$). In rTOF, the mechanisms underlying diastolic dysfunction involve reduced active suction force, which correlates with reduced LV deformation in all directions.

Keywords Tetralogy of Fallot · Intraventricular pressure gradient · Diastolic dysfunction · Echocardiography

Electronic supplementary material The online version of this article (doi:10.1007/s00380-017-1011-6) contains supplementary material, which is available to authorized users.

✉ Ken Takahashi
kentaka@juntendo.ac.jp

¹ Department of Pediatrics and Adolescent Medicine, Juntendo University, Graduate School of Medicine, 2-1-1 Hongo, Bunkyo-ku, Tokyo 113-8421, Japan

² Department of Pediatrics, Juntendo University, Faculty of Medicine, Tokyo, Japan

³ Department of Cardiovascular Surgery, Juntendo University, Faculty of Medicine, Tokyo, Japan

⁴ Department of Pediatric Cardiology, Shizuoka Children's Hospital, Shizuoka, Japan

⁵ Department of Cardiovascular Surgery, Cardiovascular Imaging Research Laboratory, Kyoto Prefectural University of Medicine, Kyoto, Japan

Introduction

In patients with repaired tetralogy of Fallot (rTOF), it is vital to detect left ventricular (LV) systolic dysfunction as early as possible, because LV systolic dysfunction is one of the strongest determinants of poor clinical outcomes in these patients [1]. LV systolic dysfunction is usually observed late after surgical correction of tetralogy of Fallot (TOF) [2], and its precise mechanisms remain unclear. Because ventricular diastolic dysfunction may predate systolic dysfunction and clinical symptoms [3], it is important to detect diastolic dysfunction both accurately and early. However, it is difficult to assess diastolic dysfunction in patients with rTOF by using conventional echocardiographic methods because such methods cannot distinguish the contribution of factors such as impaired myocardial relaxation, decreased recoil attributable to a stiffer

ventricle, and dyssynchronous ventricular relaxation [4]; moreover, conventional echocardiographic measurements do not account for key features noted in patients with rTOF, including abnormal muscle structure, presence of an artificial patch, and abnormal pre- and after-load of ventricles [1, 3, 4].

The suction force that sucks blood from the left atrium (LA) into the LV during early diastole correlates with the tau index and represents the gold-standard indicator of diastolic function [5], where it plays a fundamental role [6–9]. This force is based on the intraventricular pressure difference (IVPD). While cardiac catheterization was previously necessary for measuring the IVPD, Greenberg et al. described a non-invasive method based on echocardiography [10]. Furthermore, assessment of IVPD in LV segments (e.g., basal or mid-to-apical IVPD) has provided new and deep insight into the mechanisms underlying diastolic function [6, 9]. Specifically, mid-to-apical IVPD was found to be an indicator of active suction force [6, 9], which is more important when assessing diastolic function in a clinical setting, while basal IVPD was mainly affected by LA pressure [9]. Despite the usefulness of segmental IVPDs for the analysis of diastolic dysfunction [6, 9, 11], to the best of our knowledge, no previous study has employed this approach for the assessment of diastolic function in patients with rTOF.

When cardiac function is assessed in the pediatric population, the size of the heart represents an important issue to be considered, as the LV in adolescents and adults is almost twice as long as the LV in infants. Popović et al. described IVPG as IVPD divided by LV length [12] and showed that, although IVPG is not completely independent from the size of the heart, it is less dependent on it than IVPD. Furthermore, because IVPD is calculated by integrating the pressure difference per unit of distance along the scan line, LV length will always impact IVPD. Therefore, when comparing cardiac function among subjects with different LV length, IVPD is not a suitable indicator. To overcome this shortcoming and facilitate the comparison of cardiac function in populations including both infants and adults, IVPG is likely to be more useful than IVPD.

In the present study, we aimed to investigate the mechanistic details of LV diastolic dysfunction in patients with rTOF. As our study included also pediatric patients, we used IVPG, rather than IVPD, to assess diastolic dysfunction. Furthermore, we obtained and analyzed segmental IVPGs, with special focus on mid-to-apical IVPG.

Materials and methods

We performed a prospective echocardiographic study of consecutive patients who visited the Department of

Pediatrics at Juntendo University Hospital between May 2013 and September 2015. The inclusion criteria were as follows: (1) rTOF, (2) age between 4 and 40 years, (3) normal sinus rhythm, (4) absence of chromosomal defects, and (5) absence within other systemic diseases. Data regarding the rTOF patients were compared with those regarding controls of within the same age and sex group. The controls were recruited from among non-cardiac patients (evaluated for non-cardiac chest pain or presenting with innocent cardiac murmurs) or local community volunteers examined at Juntendo University or Shizuoka Children's Hospital. The inclusion criteria for the controls were: no history of cardiovascular disease, normal sinus rhythm on electrocardiography, and normal echocardiographic findings. The study was approved by our local institutional review board. Written, informed consent for participation was obtained from all participants or their legal guardians.

Echocardiography

All subjects underwent full echocardiography performed using a GE Vivid E9 device (GE Healthcare, Milwaukee, WI, USA) equipped with an S6 or M5S probe. For each plane, three consecutive cardiac cycles were acquired while the participant held their breath at end-expiration. In younger children, we selected three cardiac cycles from the end-expiration phase. LV end-diastolic volume, end-systolic volume, and ejection fraction were calculated with the modified Simpson method using the measurements obtained in the apical two- and four-chamber views. The mitral inflow E-wave, A-wave, *E/A* ratio, duration from the onset of the Q-wave to aortic valve closure, and mitral valve opening were measured using pulse-wave Doppler. The peak myocardial velocities during early diastole (e') were measured at the mitral lateral annulus by using tissue Doppler imaging. The pressure gradient at the right ventricular outflow tract was estimated based on the peak continuous-wave Doppler velocity. The right ventricular end-diastolic area, end-systolic area, and fractional area change were measured as described in the relevant guidelines [13]. In addition, color M-mode measurements were obtained using the apical four-chamber view [7, 10]. Three LV short-axis planes at the basal, mid, and apical levels were acquired at frame rates of 75–115 frames/s. For each plane, three consecutive cardiac cycles were acquired and stored digitally for offline analysis using the EchoPAC system version 108.1.4 (GE Healthcare, Milwaukee, WI, USA).

Measurements of LV deformation

The following parameters characterizing myocardial deformation were measured according to a protocol described in detail elsewhere [14]: peak twist, as the net difference

between basal and apical rotation; untwisting rate during early diastole; peak circumferential strain; and peak longitudinal strain. We calculated peak torsion as peak twist divided by LV length. We also calculated the peak untwisting rate normalized by LV length.

Measurements of IVPGs

For the measurement of IVPG, color M-mode images were analyzed with an in-house code written in MATLAB (The MathWorks, Natick, MA, USA) using the following image-processing algorithm (Fig. 1):

$$(\partial P)/(\partial s) = -\rho \cdot ((\partial v)/(\partial t) + v \cdot (\partial v)/(\partial s)). \quad (1)$$

The images were reconstructed using a de-aliasing technique. In Eq. (1), P is the pressure, ρ is a constant representing the density of blood (1060 kg/m^3), v is the transmitral flow velocity, s is the position along the scan line (i.e., a line along the transmitral flow where the color Doppler M-mode measurements were taken), and t is the time. The relative pressures within the region of interest can be calculated from the reconstructed velocity field [6]. At each point along the scan line, the relative pressure was expressed as the difference between the pressure at that position and the

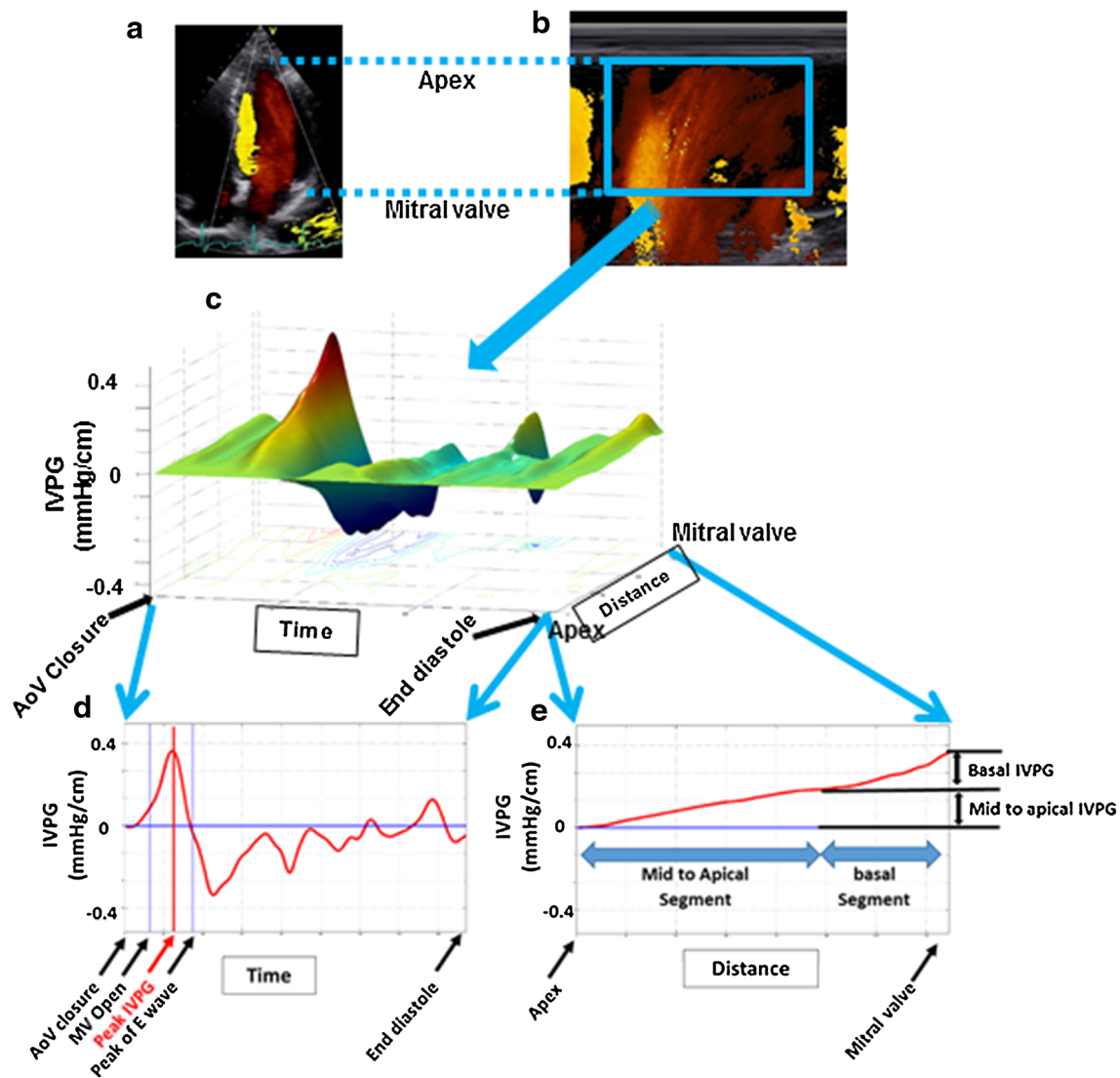


Fig. 1 Calculation of the intraventricular pressure gradient (IVPG). From the four-chamber view showing mitral inflow (a), the corresponding color M-mode Doppler image is captured (b) with the cursor parallel to the mitral inflow in an apical four-chamber view. The zero line of the Nyquist limit for two-dimensional color Doppler imaging is placed on the lower edge of the scale, and the Nyquist

limit was set at 30% above the peak E wave velocity to mitigate the aliasing phenomenon. Euler's equation, shown in Eq. (1), was used to calculate the intraventricular pressure difference at each point. A three-dimensional temporal and spatial profile of the IVPG is generated (c). Subsequently, the total IVPG (d) and segmental IVPGs (e) in early diastole are identified

pressure at the position of the mitral annulus at aortic valve closure. By calculating the line integral along the scan line, the temporal profile of the LV apex pressure relative to the LA pressure was obtained. Subsequently, the peak IVPD from the mitral valvular annulus to the LV apex was calculated as described in detail elsewhere [6, 7, 10], via a protocol previously validated against direct measurements using micromanometers [7, 10]. All data were measured from at least three beats, and the mean values were used for the final analysis. Because our study population included participants from three age groups and the LV length was almost twice as high in adults than in children, we calculated the IVPG as IVPD divided by LV length [12].

The total IVPG was divided into the basal and mid-to-apical IVPG (Fig. 2). The basal segment was defined as the first third of the LV length from the mitral valve to the LV apex; the remaining segment, which measured two-thirds of the LV length, was defined as the mid-to-apical segment.

We applied this approach because some of our patients were children, and therefore, the ventricular space could only be divided using relative distances. For comparison, previous studies that included only adults defined the basal segment as the first 2 cm from the mitral valve [6, 9], which would have been inappropriate in our pediatric participants. To quantify the characteristics of segmental IVPGs, the values were expressed as percentages of segmental IVPG from the total IVPG (i.e., as basal IVPG/total IVPG · 100 and mid-to-apical IVPG/total IVPG · 100).

Grouping

The study population was stratified according to age: the groups of children with rTOF (TOF1) or without rTOF (Control 1) included participants aged 4–9 years; the groups of adolescents with rTOF (TOF2) or without rTOF (Control 2) included participants aged 10–15 years; and the

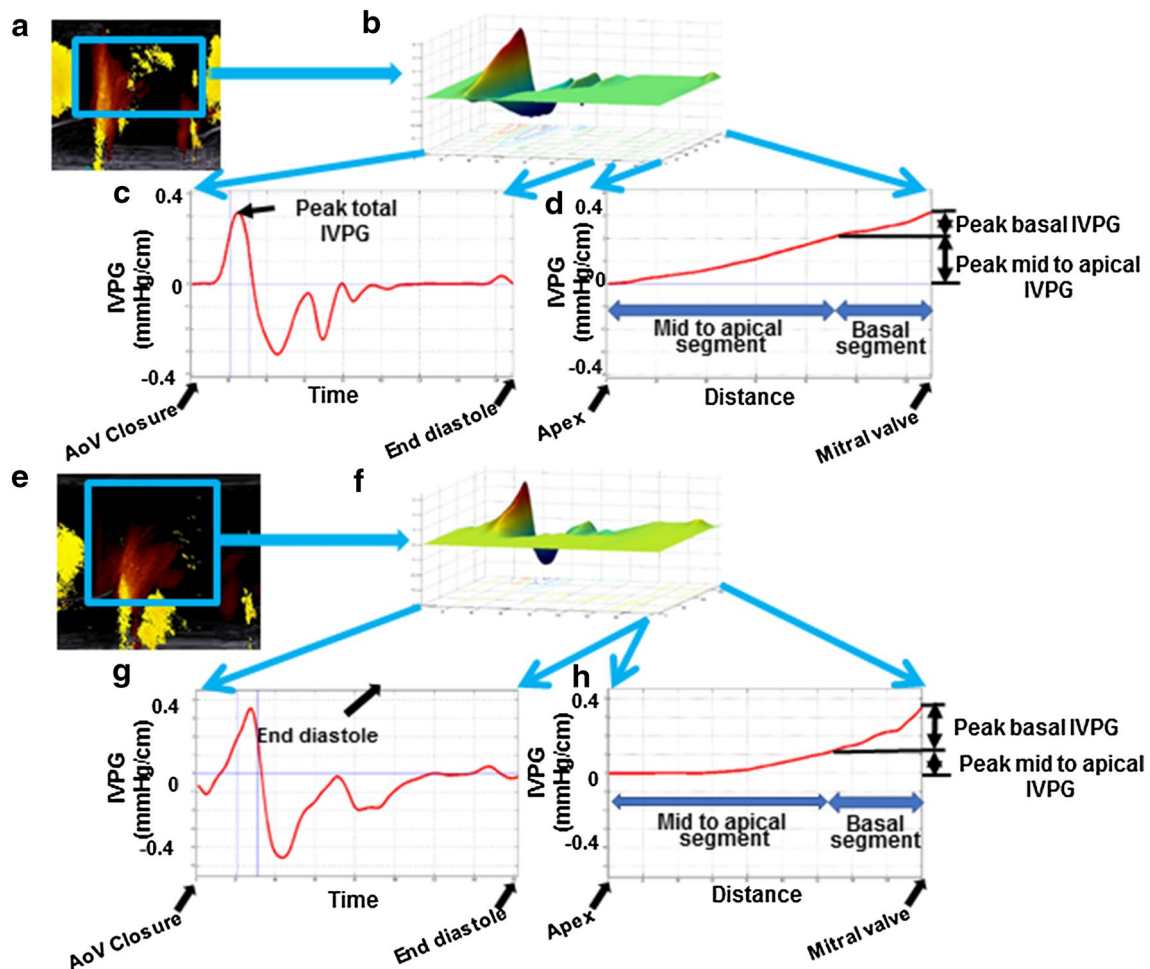


Fig. 2 Examples of intraventricular pressure gradients (IVPGs) in normal controls (a–d) and in patients with rTOF (e–h). In normal controls, the mid-to-apical IVPG is maintained (d). However, the

IVPG decreased rapidly in the basal segments, and a reduced mid-to-apical IVPG was observed in rTOF patients with very small apical IVPG (h). *rTOF* repaired tetralogy of Fallot, *AoV* aortic valve

groups of adults with rTOF (TOF3) or without rTOF (Control 3) included participants aged 16–40 years.

Statistical analysis

All data are expressed as means \pm standard deviations. After evaluating data for normality, between-group differences were assessed using one-factor analysis of variance with a post hoc Tukey–Kramer comparison test for data with normal distributions or with the Steel–Dwass test for data with non-normal distributions. The correlation between IVPGs and each variable was evaluated using the Spearman correlation coefficient, which was expressed as ρ , as some values showed non-normal distributions. For the qualitative variables, Fisher's exact test was used, as the expected values in the cross tables were below 5. To

estimate intra-observer reliability for IVPG measurements, randomly selected 5 patients and 5 controls were examined in the same manner. Two independent observers analyzed the same images, and one blinded observer repeated the analysis on a separate day. Bland–Altman limits of agreement analysis was used for assessing intra-observer and inter-observer reliability. Statistical significance was set at $p < 0.05$. Analyses were performed using JMP[®] version 8.1 (SAS Institute Inc., Cary, NC, USA).

Results

The baseline characteristics and results of the conventional echocardiographic measurements of the 38 patients with rTOF and 101 controls included in the

Table 1 Baseline characteristics and basic measurements

	TOF1 (<i>n</i> = 12)	TOF2 (<i>n</i> = 13)	TOF3 (<i>n</i> = 13)	Control 1 (<i>n</i> = 32)	Control 2 (<i>n</i> = 33)	Control 3 (<i>n</i> = 36)
Age (years)	7.0 \pm 1.3	13.0 \pm 1.2 [†]	24.2 \pm 7.1 ^{††,§§}	7.7 \pm 1.3	12.4 \pm 1.3 ^{††}	25.7 \pm 5.4 ^{††,§§}
Male/female	6/6	8/5	4/9	19/12	17/16	18/18
Body height (cm)	115 \pm 9	153 \pm 8 ^{††}	160 \pm 11 ^{††}	122 \pm 9	151 \pm 8 ^{††}	166 \pm 9 ^{††,§§}
Body weight (kg)	19.3 \pm 4.0	46.8 \pm 11.2 ^{††}	56.3 \pm 8.4 ^{††,§}	24.1 \pm 4.5	43.8 \pm 7.4 ^{††}	59.8 \pm 10.9 ^{††,§§}
Body surface area (m ²)	0.79 \pm 0.11	1.41 \pm 0.19 ^{††}	1.58 \pm 0.15 ^{††}	0.90 \pm 0.11	1.36 \pm 0.13 ^{††}	1.66 \pm 0.19 ^{††,§§}
Heart rate (bpm)	81.0 \pm 15.9	69.0 \pm 7.1 [†]	58.3 \pm 8.0 ^{††,§}	76.1 \pm 10.4	69.7 \pm 10.8	61.2 \pm 8.1 ^{††,§}
Systolic blood pressure (mmHg)	94.7 \pm 7.0	99.2 \pm 12.6	113.8 \pm 11.6 ^{††,§}	99.9 \pm 9.3	106.2 \pm 9.9 ^{††}	118.1 \pm 12.0 ^{††}
Diastolic blood pressure (mmHg)	50.0 \pm 6.9	55.8 \pm 6.8 ^{††}	66.1 \pm 9.9 ^{††}	54.0 \pm 8.3	59.0 \pm 9.2 ^{††}	70.1 \pm 9.6 ^{††,§§}
LV length (cm)	5.71 \pm 0.57	7.54 \pm 0.51 ^{††}	7.62 \pm 0.63 ^{††}	5.78 \pm 0.51	7.10 \pm 0.63 ^{††}	7.90 \pm 0.78 ^{††,§§}
QRS duration (ms)	124 \pm 24 ^{**}	121 \pm 27 [*]	134 \pm 35 ^{**}	92 \pm 8.0	96 \pm 12	97 \pm 13
LV EDV/BSA (ml/m ²)	46.4 \pm 6.9	52.4 \pm 17.2	45.8 \pm 8.4	44.5 \pm 9.7	46.6 \pm 12.6	49.0 \pm 14.6
LV ESV/BSA (ml/m ²)	15.6 \pm 2.5	17.3 \pm 6.6	16.3 \pm 4.2	14.9 \pm 4.4	15.5 \pm 4.8	17.9 \pm 5.9
LV ejection fraction (%)	66.1 \pm 3.3	67.6 \pm 4.2	64.4 \pm 5.7	66.7 \pm 3.7	66.9 \pm 4.0	63.3 \pm 4.5 ^{†,§}
<i>E</i> (m/s)	1.20 \pm 0.20 [*]	1.29 \pm 0.10 ^{**}	1.01 \pm 0.23 ^{†,§§}	1.02 \pm 0.13	1.07 \pm 0.17	0.91 \pm 0.14 [§]
<i>A</i> (m/s)	0.50 \pm 0.18	0.44 \pm 0.08	0.44 \pm 0.08	0.45 \pm 0.09	0.50 \pm 0.13	0.48 \pm 0.10
<i>E/A</i> ratio	2.71 \pm 1.12 ^{**}	2.97 \pm 0.72 [*]	2.42 \pm 0.70	2.34 \pm 0.57	2.24 \pm 0.55	1.98 \pm 0.55
<i>e'</i> lateral (cm/s)	14.4 \pm 3.9 [*]	17.2 \pm 4.8	15.1 \pm 3.1	18.9 \pm 2.4	18.8 \pm 3.4	18.0 \pm 2.8
<i>E/e'</i> ratio	9.20 \pm 3.92 ^{**}	8.09 \pm 2.37 [*]	6.93 \pm 2.03 ^{*,†}	5.48 \pm 1.01	5.83 \pm 1.22	5.13 \pm 0.94
RV EDA/BSA (cm ² /m ²)	14.8 \pm 4.0 ^{**}	14.1 \pm 3.1 [*]	11.4 \pm 1.7 [*]	10.5 \pm 2.9	10.1 \pm 3.6	7.9 \pm 2.6 ^{†,§}
RV ESA/BSA (cm ² /m ²)	6.7 \pm 3.1	6.6 \pm 1.8	5.3 \pm 1.3	5.0 \pm 1.8	5.0 \pm 2.2	3.8 \pm 1.7
RV fractional area change (%)	55.7 \pm 11.3	53.2 \pm 7.2	53.1 \pm 8.9	53.1 \pm 9.1	52.5 \pm 8.1	52.7 \pm 9.0
TAPSE (mm)	14.7 \pm 3.4 ^{**}	16.3 \pm 2.9 ^{**}	15.6 \pm 3.0 ^{**}	19.2 \pm 2.1	21.0 \pm 3.9	21.5 \pm 2.7 [†]
MAPSE (mm)	14.0 \pm 3.0	15.8 \pm 2.5	14.7 \pm 2.7	13.0 \pm 1.9	14.5 \pm 2.0 [†]	14.7 \pm 1.6

The study population was composed of TOF patients and normal controls, and was stratified according to age group as follows: TOF1 and Control 1, 4–9 years; TOF2 and Control 2, 10–15 years; and TOF3 and Control 3, 16–40 years

TOF tetralogy of Fallot, LV left ventricle, EDV end-diastolic volume, ESV end-systolic volume, BSA body surface area, RV right ventricle, EDA end-diastolic area, ESA end-systolic area

* $p < 0.05$ and ** $p < 0.001$ refer to comparisons between TOF and controls from the same age group; † $p < 0.05$ and †† $p < 0.001$ refer to comparisons between TOF1 and TOF2 or TOF3, or between Control 1 and Control 2 or Control 3; § $p < 0.05$ and §§ $p < 0.001$ refer to comparisons between TOF2 and TOF3, or between Control 2 and Control 3

Table 2 Patient characteristics

Quantitative data	TOF1	TOF2	TOF3	
Age at repair (year)	1.5 ± 0.5	1.4 ± 0.5	2.6 ± 1.2 ^{†,§}	–
Duration from the repair (year)	5.5 ± 1.5	11.7 ± 1.2 ^{††}	21.6 ± 6.3 ^{††,§§}	–
RVOT pressure gradient (mmHg)	17.8 ± 13.9	28.7 ± 12.4	21.2 ± 9.7	–
Qualitative data	TOF1	TOF2	TOF3	<i>p</i>
Transannular patch (TAP), <i>n</i> (%)	8 (66.7)	9 (69.2)	8 (66.7)	1.000
Non transannular patch, <i>n</i> (%)	4 (33.3)	1 (7.7)	5 (41.7)	0.157
Rastelli, <i>n</i> (%)	0 (0)	3 (23.1)	0 (0)	0.092
Previous shunt palliation, <i>n</i> (%)	5 (41.7)	3 (23.1)	4 (33.3)	0.620
Pulmonary regurgitation ≥ moderate, <i>n</i> (%)	9 (75.0)	9 (69.2)	8 (66.7)	1.000
NYHA class ≥ II (%)	0	0	0	1.000

TOF tetralogy of Fallot, RVOT right ventricular outflow tract, NYHA New York Heart Association

[†] $p < 0.05$ and ^{††} $p < 0.001$ refer to comparisons between TOF1 and TOF2 or TOF3; [§] $p < 0.05$ and ^{§§} $p < 0.001$ refer to comparisons between TOF2 and TOF3

study are listed in Table 1. The detailed characteristics of the patients who underwent rTOF are listed in Table 2. In terms of cardiac dysfunction, all patients were classified as having New York Heart Association functional class I without any clinical symptoms.

IVPG measurements

Representative data collected in normal controls and in patients with rTOF are shown in Fig. 2. An overview of the total and segmental IVPG measurements is provided in Fig. 3 (see also supplementary Table 1). Regarding the relationship between IVPG and age, the total IVPG did not differ significantly between rTOF patients and controls. Although total IVPG was smaller in adults with rTOF than in children with rTOF (TOF3 vs. TOF1), no such difference was noted among controls. For each age group, basal IVPG was higher in patients with rTOF than in controls. The mid-to-apical IVPG in adolescents and adults were lower among patients with rTOF than among controls (TOF2 vs. Control 2; TOF3 vs. Control 3; respectively). Interestingly, mid-to-apical IVPG was lower in adults with rTOF than in children with rTOF (TOF3 vs. TOF1). The % of mid-to-apical IVPG was significantly smaller in patients with rTOF than in controls for all age groups. Furthermore, the % of mid-to-apical IVPG was significantly smaller in adults with rTOF than in children with rTOF (TOF3 vs. TOF1), although no such difference was noted among controls. The % of basal IVPG was significantly larger in patients with rTOF than in controls for all age groups. Moreover, the % of basal IVPG was significantly larger in adults with rTOF than in children with rTOF (TOF3

vs. TOF1), while no such difference was noted among controls.

LV deformation parameters

Myocardial deformation measurements are listed in Table 3. Torsion and untwisting rate in absolute values were significantly smaller in children and adolescents with rTOF than in controls (TOF1 vs. Control 1; TOF2 vs. Control 2, respectively). The absolute value of the circumferential strain in adolescents was smaller among patients with rTOF than among controls (TOF2 vs. Control 2). The absolute value of longitudinal strain in both adolescents and adults was significantly smaller in patients with rTOF than in controls (TOF2 vs. Control 2; TOF3 vs. Control 3; respectively). In each age group, neither the circumferential nor the longitudinal strain rate differed between patients with rTOF and controls.

Relationship between LV deformation and inflow parameters and IVPGs

The statistical descriptors of the relationship between IVPGs and other parameters in the overall patient population are listed in Table 4. In all age groups, both torsion and untwisting rate normalized by LV length correlated only with mid-to-apical IVPG, and not with basal IVPG. As the value of the untwisting rate was negative, the correlation coefficient between the untwisting rate and mid-to-apical IVPG was negative. Similarly, circumferential and longitudinal strain correlated only with mid-to-apical IVPG, and not with basal IVPG. As the values of these parameters were negative, their

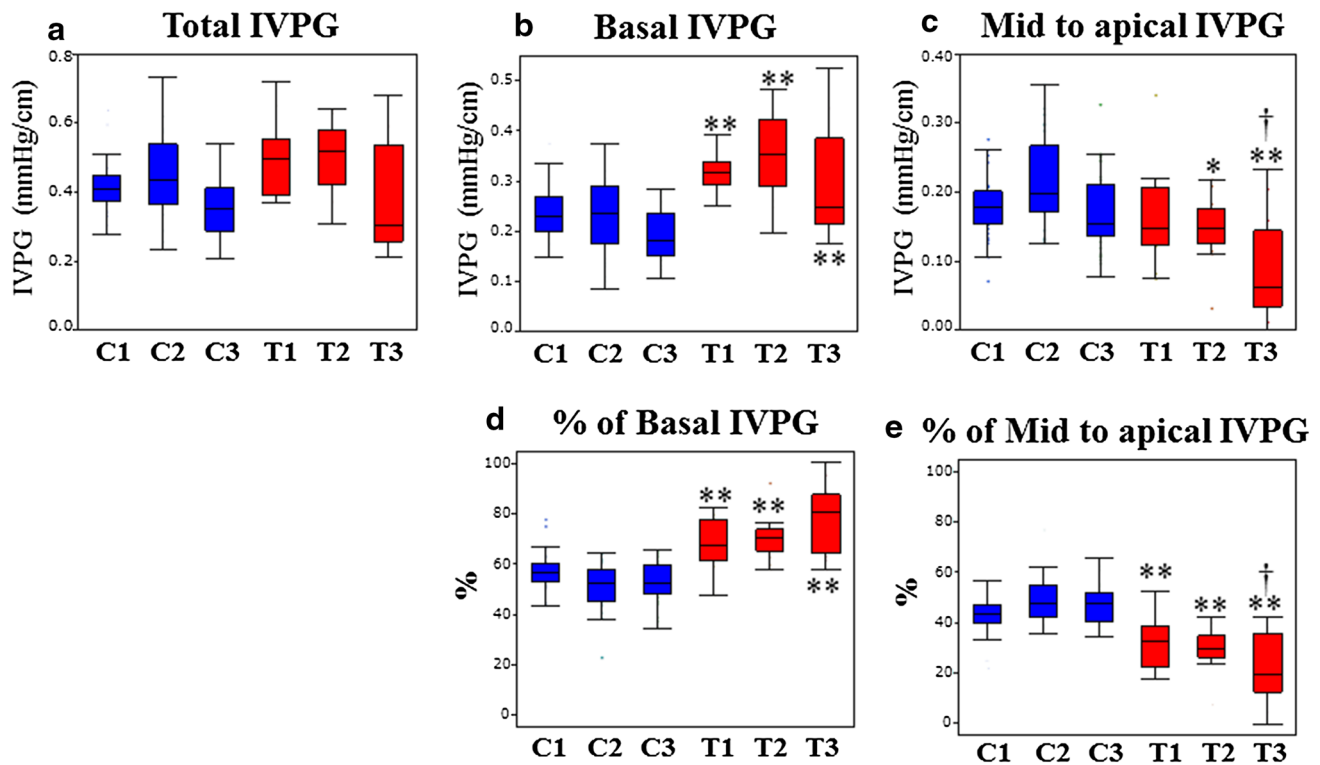


Fig. 3 Box plots of the distribution of values for intraventricular pressure gradients (IVPGs). Data regarding patients with repaired tetralogy of Fallot (*red boxes*, T1–3) and normal patients (*blue boxes*, C1–3) were stratified according to age group as follows: T1 and C1, 4–9 years; T2 and C2, 10–15 years; and T3 and C3, 16–40 years.

* $p < 0.05$ and ** $p < 0.001$ refer to comparisons between patients and controls from the same age group (i.e., T1 vs. C1, T2 vs. C2, and T3 vs. C3); † $p < 0.05$ refers to comparisons between T1 and T2 or T3, or between C1 and C2 or C3

Table 3 Myocardial deformation measurements

	TOF1 ($n = 12$)	TOF2 ($n = 13$)	TOF3 ($n = 13$)	Control 1 ($n = 32$)	Control 2 ($n = 33$)	Control 3 ($n = 36$)
Twist ($^{\circ}$)	$8.0 \pm 3.4^*$	$7.4 \pm 4.0^{**}$	8.6 ± 5.3	9.1 ± 4.5	$13.6 \pm 3.2^{\dagger\dagger}$	11.8 ± 4.8
Untwisting rate ($^{\circ}/s$)	$-87.6 \pm 36.7^*$	$-68.0 \pm 32.1^*$	-74.0 ± 32.8	-93.0 ± 36.5	-111.6 ± 27.8	-95.9 ± 33.3
Torsion ($^{\circ}/cm$)	1.38 ± 0.5	$0.98 \pm 0.54^{**}$	1.15 ± 0.74	1.59 ± 0.81	1.91 ± 0.46	1.50 ± 0.62
Untwisting rate normalized by LV length ($^{\circ}/s/cm$)	-14.5 ± 6.5	$-9.0 \pm 4.2^*$	-9.8 ± 4.5	-16.3 ± 6.8	15.5 ± 4.3	$-12.2 \pm 4.3^{\dagger}$
CS (%)	-16.1 ± 3.8	$-13.9 \pm 3.5^*$	-15.0 ± 3.0	-16.7 ± 2.9	-17.6 ± 2.7	-16.5 ± 3.0
LS (%)	-17.7 ± 2.4	$-13.8 \pm 2.8^{*\dagger\dagger}$	$-14.0 \pm 3.0^*$	-18.8 ± 1.6	$-16.7 \pm 2.1^{\dagger}$	$-16.8 \pm 2.1^{\dagger}$

The study population was composed of TOF patients and normal controls, and was stratified according to age group as follows: TOF1 and Control 1, 4–9 years; TOF2 and Control 2, 10–15 years; and TOF3 and Control 3, 16–40 years

TOF tetralogy of Fallot, LV left ventricle, IVPD intraventricular pressure difference, IVPG intraventricular pressure gradient, CS circumferential strain, LS longitudinal strain

* $p < 0.05$ and ** $p < 0.001$ refer to comparisons between TOF and controls from the same age group; † $p < 0.05$ and †† $p < 0.001$ refer to comparisons between TOF1 and TOF2 or TOF3, or between Control 1 and Control 2 or Control 3; § $p < 0.05$ and §§ $p < 0.001$ refer to comparisons between TOF2 and TOF3, or between Control 2 and Control 3

correlation coefficient describing the relationship with mid-to-apical IVPG was negative. The peak E and E/e' correlated only with the total and basal IVPG, but not

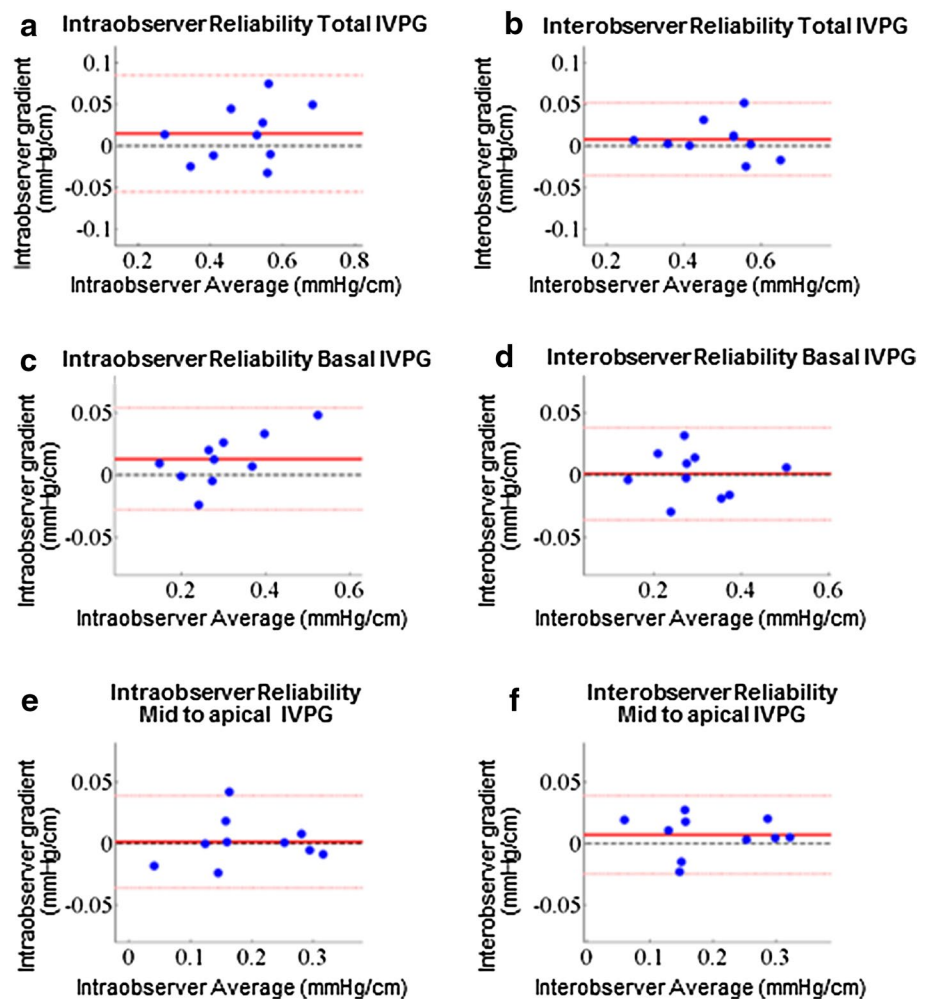
with mid-to-apical IVPG. Interestingly, QRS duration correlated positively with basal IVPG and negatively with mid-to-apical IVPG.

Table 4 Relationship between IVPGs and other parameters

	Total IVPG		Basal IVPG		Mid-to-apical IVPG	
	ρ	p	ρ	p	ρ	p
Torsion ($^{\circ}$ /cm)		0.330	–	0.658	0.245	0.005
Untwisting rate normalized by LV length ($^{\circ}$ /s/cm)		0.267		0.836	–0.223	0.010
CS (%)		0.078		0.762	–0.200	0.018
LS (%)	–0.184	0.030		0.271	–0.233	0.006
E (cm/s)	0.457	<0.001	0.503	<0.001		0.124
e'		0.163		0.847	0.254	0.003
E/e'	0.178	0.037	0.303	<0.001		0.212
QRS duration (ms)		0.621	0.227	0.009	–0.227	0.009

TOF tetralogy of Fallot, *LV* left ventricle, *IVPD* intraventricular pressure difference, *IVPG* intraventricular pressure gradient, *CS* circumferential strain, *CSR* circumferential strain rate, *LS* longitudinal strain, *LSR* longitudinal strain rate

Fig. 4 Bland–Altman plots depicting intra-observer and inter-observer reliability for the measurement of intraventricular pressure gradient (IVPG) values. Total IVPG (a, b), basal IVPG (c, d), and mid-to-apical IVPG (e, f) were measured in 10 subjects



Intra- and inter-observer variabilities

Bland–Altman analyses indicated excellent intra- and inter-observer reliabilities for the measurement of total,

basal, and mid-to-apical IVPG (Fig. 4). Intra- and inter-observer reliabilities were excellent for total, basal, and mid-to-apical IVPG.

Discussion

Mechanisms to create mid-to-apical IVPG

Although the total IVPG did not differ significantly between patients with rTOF and controls, segmental IVPG did. Therefore, it is worth to consider the role of each segment for diastolic function. The first concern is which segment creates the active suction force, as this is an important part of diastolic function [6, 9] and it correlates with the tau index [8]. Previous reports have focused on segmental IVPD in an effort to analyze the mechanisms underlying this force. Steine et al. [5] showed that, in an experimental model of ischemia, the peak early diastolic IVPD was decreased only in the apical portion, with abnormal LV motion, suggesting that the force acted only in the apical segment. Several reports also suggested a similar mechanism of reduced suction force in the apical segment in patients with diastolic dysfunction [5, 6]. The second concern refers to the factors affecting the magnitude of the suction force. The major determinant of diastolic suction is the elastic energy stored during systole [15–17]. Nikolic et al. [15] showed that the suction volume from the LA to the LV during diastole was directly related to the magnitude of the LV elastic recoil as a potential energy stored during systole. The circumferential and longitudinal strains reflect the magnitude of LV deformation and are related to the elastic recoil in the circumferential and longitudinal directions, although they show after-load dependency [18]. In our study, the values of the circumferential and longitudinal strains correlated only with mid-to-apical IVPG, and not with basal IVPG. Based on the theories described above, these correlations are considered to be very reasonable.

Besides the strain, torsional deformation is also considered to play an important role in LV diastolic function to create active suction. Systolic torsional deformation is one of the mechanisms by which potential energy is stored during ejection, in the form of a global LV “spring” [8]; this energy is promptly released during the isovolumetric relaxation time and early diastole, and can be estimated as the peak untwisting rate, which is proportional to the tau index and IVPD [8]. We found that the torsion and untwisting rate were lower in rTOF patients than in controls, which is consistent with the findings of previous studies [14, 19], and moreover showed a significant correlation with mid-to-apical IVPG. Therefore, reduced torsional deformation is also considered an important causative factor of diastolic dysfunction in rTOF.

Furthermore, LV dyssynchrony was reported in patients with rTOF and right bundle branch block, which is associated with a reduction in both regional

and global LV function and indicates a close association between QRS prolongation and LV dysfunction or asynchrony [20]. As dyssynchronous motion of the LV causes impaired relaxation and elongated tau index [21], it may also decrease mid-to-apical IVPG, which may explain why mid-to-apical IVPG correlated negatively with QRS duration.

Mechanisms of elevation of basal IVPG

Unlike mid-to-apical IVPG, basal IVPG was higher in rTOF patients than in controls for all age groups. Patients with rTOF are speculated to have abnormal LV diastolic function with abnormally high E/e' [4, 22], which is associated with elevated LA pressure [22]. Iwano et al. [9] concluded that, in patients with diastolic heart failure, basal IVPD was preserved because of an increase in LA pressure, and this basal IVPD maintained the peak E despite reduced LV suction. Our data showed that both E and E/e' correlated only with basal IVPG, and not with mid-to-apical IVPG, suggesting that elevation of basal IVPG in rTOF was indeed caused by elevated LA pressure, although the elevation of LA pressure was thought to be very small.

Clinical implications

In patients with TOF, the extent of LV deformation may decrease for a variety of reasons such as pressure overload [14], volume overload of the right ventricle with unfavorable ventricular–ventricular interactions [19], abnormal muscle fiber structure [23], duration and severity of preoperative cyanosis, cardiopulmonary bypass, patching of the ventricular septal defect, myocardial fibrosis, and ventricular dyssynchrony [2, 24, 25]. Regarding LV deformation parameters and clinical outcomes in patients with rTOF, Diller et al. recently showed that conventional echocardiographic parameters such as EF and E/e' were not useful predictors, whereas longitudinal strain was one of the strongest predictors [1]. On the contrary, Orwat et al. reported that, in young patients with TOF (median age, 16 years), the strongest prognostic marker was circumferential strain [26]. Therefore, it may be considered that the usefulness of circumferential and longitudinal strains as indicators of clinical outcome has been confirmed.

We found that in adolescents and adults patients with rTOF, mid-to-apical IVPG represented approximately two-thirds and one half, respectively, of the values noted in normal controls within the same age group, although the magnitude of the difference was much smaller for strain and torsion parameters than for mid-to-apical IVPG. Even if the decrease in the value of each cardiac deformation parameter

is small, the magnitude of decrease in mid-to-apical IVPG will be amplified because deviations in LV deformation parameters are expected to cause a decrease in mid-to-apical IVPD. Importantly, prolongation of QRS duration has been reported to increase the risk for adverse clinical outcomes in patients with rTOF [27]. As the prolongation of QRS duration may contribute to the decrease in mid-to-apical IVPG, as described above, mid-to-apical IVPG may be a more sensitive indicator of LV systolic dysfunction and clinical outcomes in patients with rTOF, potentially providing superior prognosis prediction compared to that offered by parameters of LV deformation. Furthermore, the decrease in LV deformation and the prolongation of QRS duration occurs mainly during adolescence and adulthood, which explains why we noted lower mid-to-apical IVPG in adolescents and adults with rTOF, but not in children rTOF. Therefore, monitoring IVPG is expected to be important for understanding and identifying those time courses when patients with TOF are to be followed more closely.

Limitations

Several potential limitations should be considered. First, although the accuracy of echocardiography-based measurement of IVPD has been validated by comparison to direct measurements using micromanometers [7, 20], such validation was not performed in studies involving human children. However, the fundamental structure and motion of the LV are thought to be the same as those in the models used for validation. Specifically, Popović et al. [12] showed the utility of IVPG data in small animals, where the size of the heart is smaller than that of human infants. Therefore, the measurement approach used in the present study is considered to be accurate. Second, as this study included a small number of patients, the conclusions may be underpowered. Studies with a larger sample size are needed before a robust conclusion can be put forth regarding the usefulness of mid-to-apical IVPG as an early marker of LV dysfunction in patients with rTOF.

Furthermore, in future studies, the dyssynchronous motion of the LV should be evaluated using new methods that can detect subclinical LV dysfunction [28].

Conclusions

Regarding the mechanisms underlying LV diastolic dysfunction, our findings suggest that patients with rTOF have reduced mid-to-apical IVPG, which indicates reduced active suction force related with reduced LV deformation. The measurement of mid-to-apical IVPG may be useful for quantifying diastolic dysfunction in

patients with rTOF. These represent new insights regarding diastolic dysfunction in patients with rTOF.

Acknowledgements We thank the staff of Shizuoka Children's Hospital for collecting the echocardiographic data of children and adults with no cardiac defects (control group).

Author contributions Article drafting, data collection/analysis/interpretation: MK. Study concept/design, critical revision of article, statistical analysis: KT. Data collection/analysis/interpretation: MY, KY, KM, NT, SS, KA. Study concept/design: MK, KN, SK, MN, KI. Critical revision of article: TS.

Compliance with ethical standards

Conflict of interest The authors declare that there is no conflict of interests.

Ethical approval All procedures performed in this study were in accordance with the ethical standards of the institutional and/or national research committee and with the 1964 Helsinki declaration and its later amendments or comparable ethical standards.

Informed consent Informed consent was obtained from all individual participants included in the study, or from their legal representatives.

References

1. Diller GP, Kempny A, Liodakis E, Alonso-Gonzalez R, Inuzuka R, Uebing A, Orwat S, Dimopoulos K, Swan L, Li W, Gatzoulis MA, Baumgartner H (2012) Left ventricular longitudinal function predicts life-threatening ventricular arrhythmia and death in adults with repaired tetralogy of Fallot. *Circulation* 125:2440–2446
2. Geva T, Sandweiss BM, Gauvreau K, Lock JE, Powell AJ (2004) Factors associated with impaired clinical status in long-term survivors of tetralogy of Fallot repair evaluated by magnetic resonance imaging. *J Am Coll Cardiol* 43:1068–1074
3. Nishimura RA, Tajik AJ (1997) Evaluation of diastolic filling of left ventricle in health and disease: Doppler echocardiography is the clinician's Rosetta Stone. *J Am Coll Cardiol* 30:8–18
4. Friedberg MK, Fernandes FP, Roche SL, Grosse-Wortmann L, Manliot C, Fackoury C, Slorach C, McCrindle BW, Mertens L, Kantor PF (2012) Impaired right and left ventricular diastolic myocardial mechanics and filling in asymptomatic children and adolescents after repair of tetralogy of Fallot. *Eur Heart J Cardiovasc Imaging* 13:905–913
5. Steine K, Stugaard M, Smiseth OA (1999) Mechanisms of retarded apical filling in acute ischemic left ventricular failure. *Circulation* 99:2048–2054
6. Ohara T, Niebel CL, Stewart KC, Charonko JJ, Pu M, Vlachos PP, Little WC (2012) Loss of adrenergic augmentation of diastolic intra-LV pressure difference in patients with diastolic dysfunction: evaluation by color M-mode echocardiography. *JACC Cardiovasc Imaging* 5:861–870
7. Yotti R, Bermejo J, Antoranz JC, Desco MM, Cortina C, Rojo-Alvarez JL, Allué C, Martín L, Moreno M, Serrano JA, Muñoz R, García-Fernández MA (2005) A noninvasive method for assessing impaired diastolic suction in patients with dilated cardiomyopathy. *Circulation* 112:2921–2929

8. Notomi Y, Popovic ZB, Yamada H, Wallick DW, Martin MG, Oryszak SJ, Shiota T, Greenberg NL, Thomas JD (2008) Ventricular untwisting: a temporal link between left ventricular relaxation and suction. *Am J Physiol Heart Circ Physiol* 294:H505–H513
9. Iwano H, Kamimura D, Fox E, Hall M, Vlachos P, Little WC (2015) Altered spatial distribution of the diastolic left ventricular pressure difference in heart failure. *J Am Soc Echocardiogr* 28:597–605
10. Greenberg NL, Vandervoort PM, Firstenberg MS, Garcia MJ, Thomas JD (2001) Estimation of diastolic intraventricular pressure gradients by Doppler M-mode echocardiography. *Am J Physiol Heart Circ Physiol* 280:H2507–H2515
11. Stewart KC, Kumar R, Charonko JJ, Ohara T, Vlachos PP, Little WC (2011) Evaluation of LV diastolic function from color M-mode echocardiography. *JACC Cardiovasc Imaging* 4:37–46
12. Popović ZB, Richards KE, Greenberg NL, Rovner A, Drinko J, Cheng Y, Penn MS, Fukamachi K, Mal N, Levine BD, Garcia MJ, Thomas JD (2006) Scaling of diastolic intraventricular pressure gradients is related to filling time duration. *Am J Physiol Heart Circ Physiol* 291:H762–H769
13. Lang RM, Badano LP, Mor-Avi V, Afilalo J, Armstrong A, Ernande L, Flachskampf FA, Foster E, Goldstein SA, Kuznetsova T, Lancellotti P, Muraru D, Picard MH, Rietzschel ER, Rudski L, Spencer KT, Tsang W, Voigt JU (2015) Recommendations for cardiac chamber quantification by echocardiography in adults: an update from the American Society of Echocardiography and the European Association of Cardiovascular Imaging. *J Am Soc Echocardiogr* 28:1–39
14. Takayasu H, Takahashi K, Takigiku K, Yasukochi S, Furukawa T, Akimoto K, Kishiro M, Shimizu T (2011) Left ventricular torsion and strain in patients with repaired tetralogy of Fallot assessed by speckle tracking imaging. *Echocardiography* 28:720–729
15. Nikolic SD, Yellin EL, Tamura K, Vetter H, Tamura T, Meisner JS, Frater RW (1988) Passive properties of canine left ventricle: diastolic stiffness and restoring forces. *Circ Res* 62:1210–1222
16. Bell SP, Nyland L, Tischler MD, McNabb M, Granzier H, LeWinter MM (2000) Alterations in the determinants of diastolic suction during pacing tachycardia. *Circ Res* 87:235–240
17. Solomon SB, Nikolic SD, Glantz SA, Yellin EL (1998) Left ventricular diastolic function of remodeled myocardium in dogs with pacing-induced heart failure. *Am J Physiol* 274:H945–H954
18. Murai D, Yamada S, Hayashi T, Okada K, Nishino H, Nakabachi M, Yokoyama S, Abe A, Ichikawa A, Ono K, Kaga S, Iwano H, Mikami T, Tsutsui H (2016) Relationships of left ventricular strain and strain rate to wall stress and their afterload dependency. *Heart Vessels*. doi:10.1007/s00380-016-0900-4
19. van der Hulst AE, Delgado V, Holman ER, Kroft LJ, de Roos A, Hazekamp MG, Blom NA, Bax JJ, Roest AA (2010) Relation of left ventricular twist and global strain with right ventricular dysfunction in patients after operative “correction” of tetralogy of fallot. *Am J Cardiol* 106:723–729
20. Abd E, Rahman MY, Hui W, Yigitbasi M, Dsebissowa F, Schubert S, Hetzer R, Lange PE, Abdul-Khaliq H (2005) Detection of left ventricular asynchrony in patients with right bundle branch block after repair of tetralogy of Fallot using tissue-Doppler imaging-derived strain. *J Am Coll Cardiol* 45:915–921
21. Wang J, Kurrelmeyer KM, Torre-Amione G, Nagueh SF (2007) Systolic and diastolic dyssynchrony in patients with diastolic heart failure and the effect of medical therapy. *J Am Coll Cardiol* 49:88–96
22. Koenigstein K, Raedle-Hurst T, Hosse M, Hauser M, Abdul-Khaliq H (2013) Altered diastolic left atrial and ventricular performance in asymptomatic patients after repair of tetralogy of Fallot. *Pediatr Cardiol* 34:948–953
23. Sanchez-Quintana D, Anderson RH, Ho SY (1996) Ventricular myoarchitecture in tetralogy of Fallot. *Heart* 76:280–286
24. Babu-Narayan SV, Kilner PJ, Li W, Moon JC, Goktekin O, Davlouros PA, Khan M, Ho SY, Pennell DJ, Gatzoulis MA (2006) Ventricular fibrosis suggested by cardiovascular magnetic resonance in adults with repaired tetralogy of fallot and its relationship to adverse markers of clinical outcome. *Circulation* 113:405–413
25. Hausdorf G, Hinrichs C, Nienaber CA, Scharck C, Keck EW (1990) Left ventricular contractile state after surgical correction of tetralogy of Fallot: risk factors for late left ventricular dysfunction. *Pediatr Cardiol* 11:61–68
26. Orwat S, Diller GP, Kempny A, Radke R, Peters B, Kühne T, Boethig D, Gutberlet M, Dubowy KO, Beerbaum P, Sarikouch S, Baumgartner H, German Competence Network for Congenital Heart Defects Investigators (2016) Myocardial deformation parameters predict outcome in patients with repaired tetralogy of Fallot. *Heart* 102:209–215
27. Gatzoulis MA, Till JA, Somerville J, Redington AN (1995) Mechano-electrical interaction in tetralogy of Fallot. QRS prolongation relates to right ventricular size and predicts malignant ventricular arrhythmias and sudden death. *Circulation* 92:231–237
28. Kim SA, Kim MN, Shim WJ, Park SM (2016) Layer-specific dyssynchrony and its relationship to the change of left ventricular function in hypertensive patients. *Heart Vessels* 31:528–534